

FREE VIBRATIONS OF RECTANGULAR SOLAR SAILS

Tina M. Morrison and Kevin D. Murphy
Department of Mechanical Engineering
University of Connecticut, Storrs, CT 06269-3139

ABSTRACT

This work examines the free vibration characteristics of rectangular solar sails. The sail is modeled as a thin elastic membrane and the booms, which support the sail, are modeled as applied tensile loads acting at the corners of the membrane. The equation of motion is derived via Hamilton's principle; a Levy solution to the compatibility equation is developed for the spatially nonuniform tension field (arising from the applied corner loads) and is used in concert with the equations of motion to examine the natural frequencies and mode shapes. These response quantities are examined as a function of the corner load angle and provide insight into the free and forced response under skewed corner loads.

INTRODUCTION

Recently, the NASA made a strategic decision to use solar sails for a variety of deep space research programs [1]. These sails, by providing a means of *non-propellant propulsion*, will have a dramatic influence on the success of these programs by leading to a significant weight reduction while maintaining spacecraft maneuverability.

A typical sail, shown in Figure 1a, is propelled through space using photon pressure provided by the sun. Because the momentum carried by a single photon is small, a large number of photons must be collected. Hence, an extremely large sail is required; sail areas on the order of 10^4 m² are typical [1]. To reduce weight, the sail substrate is made of lightweight Kapton with a thickness on the order of 12 μ m. Because of their size and material properties, solar sails possess negligible flexural stiffness and may be modeled as a large membrane. The boundaries of the membrane are free, except at the corners where the booms exert a concentrated load, as shown in Figure 1b.

Because vibrations may hamper maneuverability and may lead to failure (ripping of the sail), it is imperative to understand the vibration characteristics of this system. In this work, a membrane model is developed in a two step process: (i) a Levy solution is obtained for the spatially

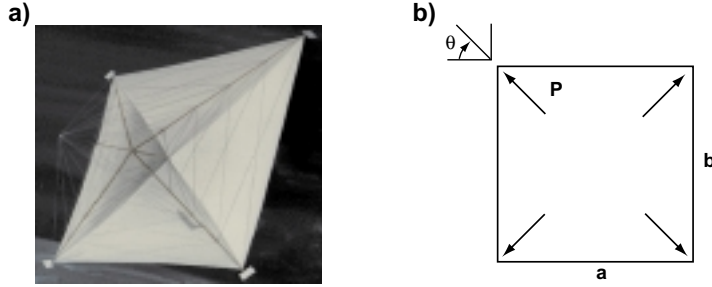


Figure 1: a) an artists rendering of a solar sail and b) the idealized geometry of the sail.

non-uniform internal tension field (created by the corner loads) [2], [3] and (ii) Hamilton's principle is used, along with the aforementioned tension field, to obtain the governing equation for the membrane. This equation is discretized in a Galerkin procedure and the free vibration eigenproblem is solved. A parametric study is undertaken and the results show that the frequencies are a sensitive function of the corner load angle. More importantly, this study serves to highlight the utility and speed of this model, indicating that it may be of substantial use in the sail design process.

MODEL DEVELOPMENT

Internal Tension Field Due to a Corner Load

In order to describe the vibration characteristics, the internal stress field resulting from the corner loads, must be quantified. This is accomplished by using a Levy solution approach as outlined in references [2] and [3]. This solution procedure is briefly described here.

To maintain compatibility between the strain field and the in-plane displacements, the following equation must be satisfied:

$$\nabla^4 \Phi = 0, \quad (1)$$

where Φ is the Airy stress function [4]. This stress function also defines the in-plane stresses:

$$\sigma_{xx} = \Phi_{,yy} \quad \sigma_{yy} = \Phi_{,xx} \quad \tau_{xy} = -\Phi_{,xy} \quad (2)$$

where $\bullet, x \equiv \partial \bullet / \partial x$. The complete stress function, Φ , is determined by a superposition of three Airy stress functions, each representing a separate loading scenario, as will be described shortly. To begin, the stress function will be defined for an arbitrary loading case shown in Fig. 2a.

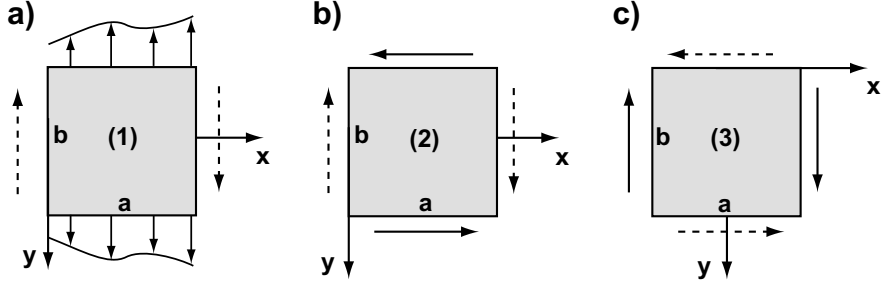


Figure 2: (a) A general loading scenario in the y -direction and the artificial edge shear that arises from Φ^1 , (b) the imposed edge shear (solid) on $y = -b/2, b/2$ and its artificial edge shear and (c) the imposed edge shear (solid) on $x = 0, a$ and its artificial edge shear.

In this loading scenario, the applied tensile edge stress at $y = \pm b/2$ may be written as a Fourier sine series

$$\sigma_{yy} = \sum_{m=1}^n A_m \sin(m\pi x/a), \quad (3)$$

where A_m is the m^{th} Fourier coefficient of the load. Only the odd terms are kept in this expansion because the modes being analyzed are symmetric about the $x = a/2$ axis. This represents the *actual applied load* and, hence, the A_m are known. Note that for overall equilibrium, there is symmetry about the $y = 0$ axis. Also, there is no shear stress present on the edges.

Because (i) the prescribed edge loading is expressed as a Fourier sine series (Equation (3)) and (ii) the Airy stress function is related to the stress via Equation (2), Φ^1 must take the form

$$\Phi_m^1(x, y) = \sum_{m=1,3,5,\dots}^{\infty} Y_m(y) \sin\left(\frac{m\pi x}{a}\right) \quad (4)$$

By substituting this into the compatibility equation, Equation (1), and taking advantage of symmetry, it can be shown that $Y_m(y) = D_{1m} \cosh(\alpha_m y) + D_{2m} y \sinh(\alpha_m y)$. Here, $\alpha_m = (m\pi/a)$ and the D_{1m} and D_{2m} are two infinite sets of unknown coefficients. These are found by satisfying the following boundary conditions:

$$\begin{aligned} \sigma_{yy}(x, b/2) &= \Phi_{,xx}^1(x, b/2) \\ \tau_{xy}(x, b/2) &= -\Phi_{,xy}^1(x, b/2) = 0. \end{aligned} \quad (5)$$

This Airy stress function properly describes the normal stresses on the edges and the zero shear stress along the edges $y = -b/2, b/2$. However,

this solution renders a nonzero shear stress along $x = 0, a$, though this shear stress does not exist physically. The stress field produced by Φ^1 is shown in Figure 2a; the artificial shear is shown in dashed arrows. This shear results from this stress function and is a mathematical artifact; it must be eliminated.

A second and third shear loading are introduced (see the solid lines in Figures 2b and 2c) to eliminate this unwanted shear on the edges. The procedure for generating the two associated stress functions Φ^2 and Φ^3 follow a similar procedure to that for Φ^1 . However, the details are omitted for the sake of brevity. The interested reader is encouraged to see reference [3]. The consequence is that the superposition of these three stress functions leads to a zero net shear while maintaining the appropriate normal stress on the edges.

For an applied load in the x -direction, the same procedure is followed (swapping x for y and vice-versa). Hence, a combined x and y loading situation may be addressed individually and the results superimposed.

Equations of Motion

In the absence of external work (i.e., for free vibrations), the governing equations are obtained using Hamilton's principle: $\int_{t_1}^{t_2} (\delta T - \delta U) dt = 0$, where T and U are the kinetic and strain energies, respectively. The internal strain energy is given by

$$U = \frac{Eh}{2} \int_0^a \int_0^b (\epsilon_{xx}^2 + \epsilon_{yy}^2) dx dy, \quad (6)$$

where the linear strains are given by $\epsilon_{xx} = u_{,x} + \frac{\sigma_{xx}}{E}$ and $\epsilon_{yy} = v_{,y} + \frac{\sigma_{yy}}{E}$; σ_{xx} and σ_{yy} are the internal stress fields due to the edge loading. The kinetic energy is

$$T = \frac{1}{2} \int_0^a \int_0^b m w_{,t}^2 dx dy, \quad (7)$$

where m is the mass per unit area. Applying Hamilton's principle, recognizing that $\sigma_{xx} = \sigma_{xx}(x, y)$ and $\sigma_{yy} = \sigma_{yy}(x, y)$, and carrying out the necessary integration by parts, leads to the following PDE governing the out-of-plane displacement, $w(x, y, t)$:

$$\left(\frac{\sigma_{xx}}{A}\right) w_{,xx} + \left(\frac{\sigma_{xx,x}}{A}\right) w_{,x} + \left(\frac{\sigma_{yy}}{A}\right) w_{,yy} + \left(\frac{\sigma_{yy,y}}{A}\right) w_{,y} = \rho w_{,tt}, \quad (8)$$

where A is the surface area. For a given loading, closed form expressions for the internal stress fields σ_{xx} and σ_{yy} may be easily obtained by applying the solution procedure of the previous section for Φ and then using Equation (2). Therefore, the only remaining unknown is $w(x, y, t)$.

Natural Frequencies and Stability

In order to examine the free vibration characteristics, the governing equation is discretized using a Galerkin procedure. The displacement field is expressed as $w(x, y, t) = \sum a_i(t)\Psi_i(x, y)$, where the expansion functions Ψ_i are the mode shapes of a free-free membrane under uniform tension [5]. Using this expansion with Galerkin's method, Equation (8) may be discretized into the following set of matrix equations:

$$[M]\ddot{\mathbf{x}} + [K]\mathbf{x} = \mathbf{0}, \quad (9)$$

where $\mathbf{x} = \{a_1, a_2, a_3, \dots\}^t$ is a vector of the modal amplitudes, $[M]$ is the mass matrix, and $[K]$ is the stiffness matrix. The natural frequencies for this system are found by assuming a solution of the form $\mathbf{x} = \mathbf{X}e^{i\omega t}$. This leads to an eigenvalue problem, which is solved numerically.

RESULTS

The point of this study was to develop a model of a rectangular solar sail and to use the model to carry out parametric studies on the vibration characteristics. The parameter to be varied here is the corner load angle, θ , see Figure 1. The particular sail under consideration is a scaled down test model being used at NASA Langley. Its dimensions are $2\text{m} \times 2\text{m} \times 12\mu\text{m}$. The magnitude of the corner load was 5N. The edge loads were simple concentrated loads; they were modeled with Dirac delta functions. Twenty terms ($m = 20$) were retained in the Fourier series in each Airy stress function and ten modes were retained in the Galerkin discretization of $w(x, y, t)$. This was sufficient to ensure that the first frequency was converged to 99.4%.

For the square membrane, the results are symmetric about $\theta = 45^\circ$ (i.e., the $45^\circ \rightarrow 90^\circ$ results will mirror those from $0^\circ \rightarrow 45^\circ$). Hence, results are presented only up to $\theta = 45^\circ$.

The frequencies of the first nine modes are shown in Figure 3 for varying corner load angles. Figure 3a shows four of the eigenvalues, though curves 1 and 2 are coincident, as are curves 3 and 4. Figure 3b shows two other eigenvalues. And finally, 3c shows the last three. There are two interesting features here. At 0° the 8^{th} loci is coincident with 9^{th} loci, but they split at 6° . The frequency path of 8^{th} eigenvalue drops relatively close to zero and then increases after 24° . The 9^{th} loci coalesces with the 7^{th} eigenvalue curve and they share a coincident eigenvalue during the remaining analysis.

The splitting of the 8^{th} and 9^{th} loci and the eventual coalescence of the 9^{th} and 7^{th} loci demonstrates some interesting behavior in their mode shapes. The two data sets, 8 and 9, share a coincident eigenvalue at 0°

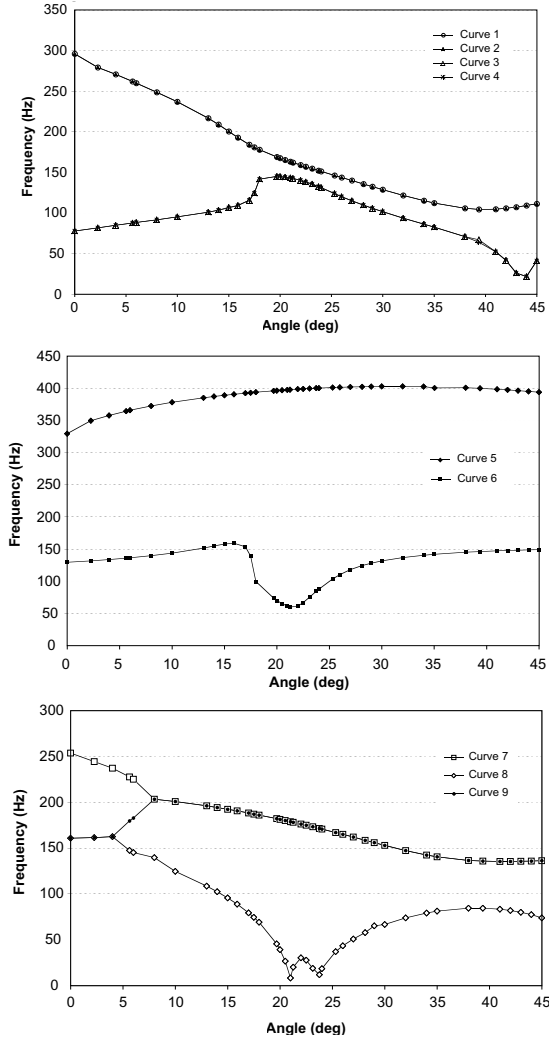


Figure 3: The first nine natural frequencies as a function of the applied corner load angle.

(160.73 Hz), 2° (161.53 Hz) and 4° (161.49 Hz). While they share the same eigenvalue, they do not share the same mode shape. As locus 9 coalesces with 7 at 8° (203.42 Hz) and they share a coincident eigenvalue for the rest of the simulation, though their mode shapes differ.

Around 20° , the 8^{th} loci approaches 0 Hz. The reason for this abrupt drop in frequency is not well understood. However, the following explanation is offered as one possibility. The natural frequency is one measure of a systems stiffness: ($\omega \approx \sqrt{k/m}$). But in these membranes, the restoring force is entirely due to the internal tension field (calculated earlier via the Levy solution). The portion of the membrane where the tension is low may coincide with a peak in the mode shape. Hence, there

is virtually no restoring force at the point of largest deflection. As a result, the effective stiffness (and the frequency) appears to be almost zero.

Summary

In this paper, a model is proposed for the study of the free vibration characteristics of rectangular solar sails. The natural frequencies of these sail change greatly but in a regular, predictable way as a function of the corner load angle. In summary, the observed results include: (i) at zero degrees, six of the first nine frequencies occur in pairs, (ii) one pair splits at 6° , (iii) another pair coalesces at 8° , and (iv) one frequency approaches zero near 24° . These results clearly indicate the predictive capability of this model and provide insight into the basic mechanics of the sail system.

ACKNOWLEDGEMENTS

The support of the NASA GSRP program (NGT-1-01025) and Dr. Keith Belvin are gratefully acknowledged.

REFERENCES

- [1] Garner, C., Leipold, M., "Developments and Activities in Solar Sail Propulsion," NASA JPC-00-0126.
- [2] Gorman, D.J., "Investigation of the Stress Distribution in Corner Tensioned Rectangular Membranes," *AIAA Journal*, 1993, **31**(12), 2361.
- [3] Morrision, T.M., Vibration Characteristics of Solar Sails, *Masters Thesis*, University of Connecticut, Storrs, CT, 2002.
- [4] Timoshenko, S.P., Goodier, J.N., *Theory of Elasticity*, 3rd Edition, McGraw-Hill, New York, 1987.
- [5] Meirovitch, L., *Analytic Methods in Vibrations*, McMillan Press, New York, 1967.